Purification and Characterization of Single-Wall Carbon Nanotubes

I. W. Chiang, B. E. Brinson, R. E. Smalley, J. L. Margrave, and R. H. Hauge*

Center for Nanoscale Science and Technology, Rice Quantum Institute and Department of Chemistry, MS-60, Rice University, 6100 Main Street, Houston, Texas 77005

Received: September 23, 2000; In Final Form: November 28, 2000

A purification method has been developed that provides for the removal of metal catalysts and impurity carbon from laser-oven-grown single-wall carbon nanotube (SWNT) material. The oxidation rate of SWNTs in air at elevated temperatures is correlated to the metal content of the sample. Sample purity is documented with SEM, TEM, electron microprobe analysis, Raman, and UV−vis−near-IR. We also note that the relative intensity of the electronic transitions in the near-infrared to the continuum absorption at 400 nm in the UV serves as a useful monitor of the perturbation of the sidewall π-electron density of SWNTs due to sidewall substitution and/or oxidation.

Introduction

Since their discovery in 1990,[1,2] carbon single-wall nanotubes (SWNTs) have attracted considerable interest because of their unique physical, chemical, and mechanical properties.[3−7] Carbon SWNTs are expected to be useful in many different fields, such as field emission displays, supercapacitors, molecular computers, and ultrahigh strength materials. However, in order to obtain the optimal performance of SWNTs in various applications, high-purity carbon SWNTs will be required.

The impurities typically found in as-prepared carbon single-wall nanotubes (SWNTs) are the metals that were used as catalysts for growth and amorphous carbon. Metals are present as nanoparticles and typically encased in carbon outer layers that make them impervious to dissolution in an acid. All purification methods attempt to remove the metal and unwanted carbon without affecting the carbon SWNTs. Different purification methods have been reported to date.[8−11] The purity of the SWNTs is typically reported in terms of the metal content and apparent particle content relative to SWNTs.

Carbon single-wall nanotubes are typically accompanied by other carbonaceous materials when synthesized using the laser oven method or arc discharge evaporation method. A number of purification methods have been developed to date. They can be categorized into four major methods: acid oxidation, gas oxidation, filtration, and chromatography. The acid reflux procedure was first described by Rinzer et al.,[12] in which raw nanotube materials are refluxed in nitric acid to oxidize the metals and impurity carbons. Other groups have employed different reaction times, temperatures, and acid concentrations, with similar results. Acid-treated nanotubes are thought to have carboxylic acid groups at the tube ends and, possibly, at defects on the sidewalls. Since functionalized SWNTs will have considerably different properties than those of pristine tubes, the extent of chemical modification achieved through the acid purification route must be carefully evaluated.

Gas phase oxidation is commonly used as the purification method for MWNT.[13−15] However, Dujardin et al. have suggested that the same purification process would destroy single-wall carbon nanotubes. Dillon et al.[16] have described an oxidation process that produces >98 wt % pure SWNTs. In their purification process, raw nanotube soot first undergoes a nitric acid refluxing process. Oxidation of the acid-treated product is then carried out in air at 550 °C for 30 min, leaving behind SWNTs having a weight of ∼20% of the initial raw material. TGA studies indicate that these purified tubes can withstand temperatures up to 600 °C in air. Zimmerman et al.[17] have discussed an oxidation with a mixture of HCl, Cl_2, and H_2O to remove unwanted carbon in raw nanotube materials. Only a small quantity (∼5 mg) of nanotubes was purified each time, and no large scale purification by this method was demonstrated.

Bandow et al.[18] have reported a procedure for a one-step SWNT purification by microfiltration in an aqueous solution in the presence of a cationic surfactant. Konstantin et al.[19] developed an ultrasonically assisted filtration method which allows the purity of nanotubes to reach >90%. Highly pure and length-selected SWNTs in aqueous solution can be obtained by column chromatography, according to Duesberg et al.[20] Limited solubility of nanotubes is the major disadvantage of size-exclusion chromatographic methods.

This study defines a cleaning procedure that provides additional removal of metal and nonnanotube carbon from SWNT samples that have been grown with the laser oven method and initially cleaned with nitric acid. The process is similar to that suggested by Dillon et al.[16] with the difference that this gas phase oxidation process is carried out at successively higher temperatures, with each step followed by an acid wash. We believe this approach preserves a larger fraction of the SWNT component of the sample.

In the course of working with SWNTs, it became obvious that there is a clear correlation between the temperature at which air oxidation of SWNTs begins and the metal content of the sample. The metal is typically present as nanoparticles with a carbon coating that varies from disordered carbon layers to graphitic shells. It is thought that low temperature oxidation can remove the more disordered carbon layer which permits removal of this metal with an acid wash. We believe it is important that this metal be removed before going to high temperature oxidation since metal nanoparticles are likely to catalyze the oxidation of SWNTs. Higher temperature oxidation

* To whom correspondence should be addressed. E-mail: hauge@rice.edu.

10.1021/jp003453z CCC: $20.00
Published on Web 01/12/2001

TABLE 1: Weight Loss and Metal Concentration in SWNTs after Purification Process

	metal atomic %[a]	weight loss[b] *(%)*
(a) as-purified Tubes@Rice SWNTs	1.71	
(b) (a) after water reflux	1.56	9.2
(c) (b) heated in 300 °C, 5% O_2/Ar	1.44	8.7
(d) (c) heated in 400 °C, 5% O_2/Ar	1.41	8.8
(e) (d) heated in 450 °C, 5% O_2/Ar	1.43	12.2
(f) (e)heated in 500 °C, 5% O_2/Ar	0.17	18.9

[a] $M_X/M_c \times 100$, where M = atomic %, X = Co + Ni, C = carbon. [b] Total weight loss from the process is 57.8%.

TABLE 2: Weight Loss after Each Process and Metal Concentration in SWNTs[a]

	(a)	(b)	(c)	(d)
Co	0.97	0.88	0.85	0.10
Ni	0.84	0.68	0.59	0.07
metal atomic %[b]	1.81	1.56	1.44	0.17
weight loss[c] *(%)*		4.25	17.07	22.94

[a] (a) As-purified Tubes@Rice SWNTs. (b) (a) water refluxed. (c) (b) heated at 300 °C in 5% O_2/Ar. (d) (c) heated at 500 °C in 5% O_2/Ar. [b] $M_X/M_c \times 100$, where M = atomic %, X = Co + Ni, C = carbon. [c] Total weight loss from the process is 44.3%.

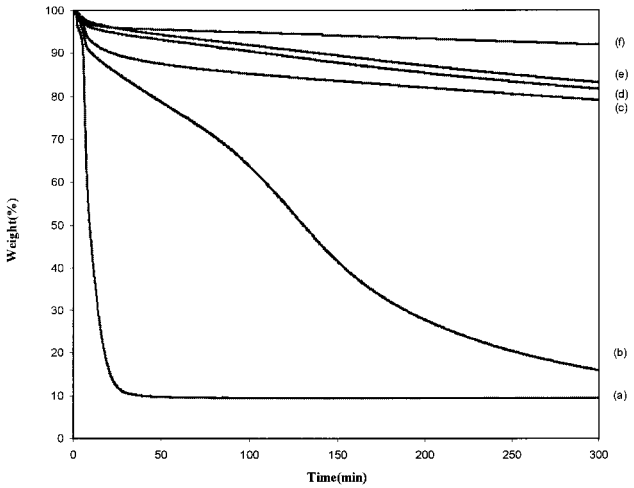

Figure 1. TGA of SWNTs in the corresponding order of purification stages: (a) as-purified Tubes@Rice SWNTs, (b) (a) after water reflux, (c) heated in 300 °C, 5% O_2/Ar, (d) heated in 400 °C, 5% O_2/Ar, (e) (d) heated in 450 °C, 5% O_2/Ar, (f) (e) heated in 500 °C, 5% O_2/Ar.

removes the more stable carbon layer on the remaining metal particles thus permitting their removal with an acid wash.

A limiting temperature near 500 °C exists where the rate of removal of the carbon layer on the metal particles is similar to the uncatalyzed, gas phase oxidation of SWNTs. At this point, any further metal removal by oxidative removal of the metal particle carbon coatings results in a large loss of SWNTs.

Sample purity is documented with SEM, TEM, and electron microprobe elemental analysis. Raman and UV−vis−near-IR spectra are also reported for the different stages of the cleaning procedure.

Experimental Procedure

In these studies, Raman spectra were obtained with a Renishaw micro-Raman spectrometer operating with a 780 nm laser. UV−vis−near-IR spectra were obtained with a Shimadzu-UV-3101 PC spectrometer. Transmission electron microscopy (JEOL 2010 TEM) was obtained using 100 kV beam energy. Thermogravimetric (TGA) data was obtained with a TA

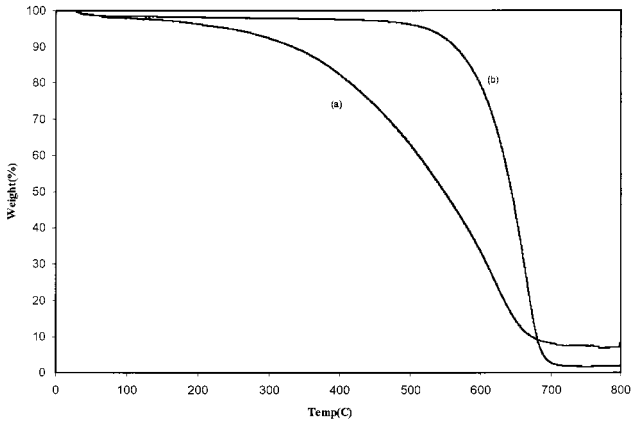

Figure 2. TGA of metal effects in oxidation: (a) Co added (to purified SWNTs), (b) two-stage purified SWNTs.

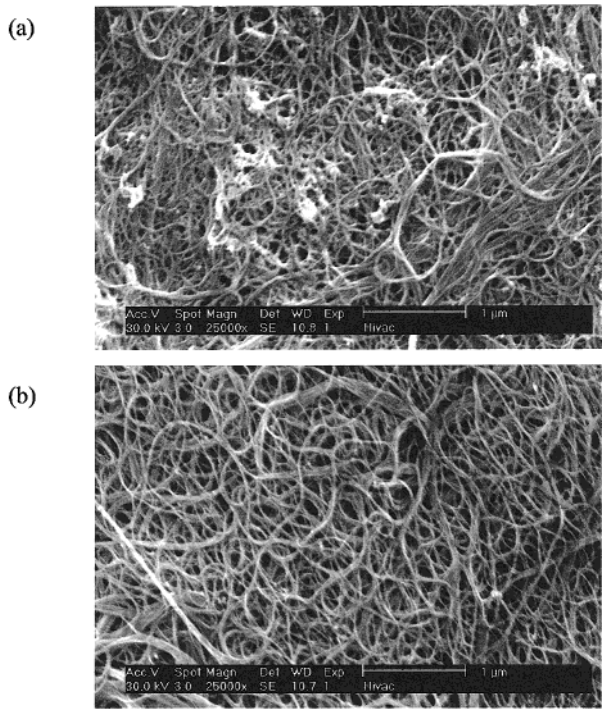

Figure 3. SEM images of SWNTs: (a) before purification (as-purified Tubes@Rice SWNTs), (b) after two-stage purification process, unannealed.

Instruments model 2960 system. Elemental analysis was obtained with a Cameca SX 50 electron microprobe equipped with four wavelength dispersive X-ray spectrometers. Raman, IR, and TGA were carried out with SWNTs in the form of buckypaper. Samples for UV−vis−near-IR were prepared by sonicating SWNTs for ∼10 min in 0.15 wt % Triton-X/D_2O solution in a cup sonicator at 55 kHz. TEM samples were prepared by sonicating SWNTs in methanol and drop drying them onto lacey carbon TEM grids.

The starting SWNT samples were obtained from Tubes@Rice[12,21] as a suspension in toluene. This suspension was filtered and washed with methanol to remove additional soluble residue left from the initial nitric acid cleaning carried out by Tubes@Rice. This left a black puffy paper (buckypaper). This paper was then refluxed in water[22,23] for approximately 2−5 h, depending on the amount of starting material. The water becomes yellowish which suggests further removal of aromatic carboxyl acids.

Two sets of metal removal studies were carried out with successive gas phase oxidation at increasing temperatures. Each

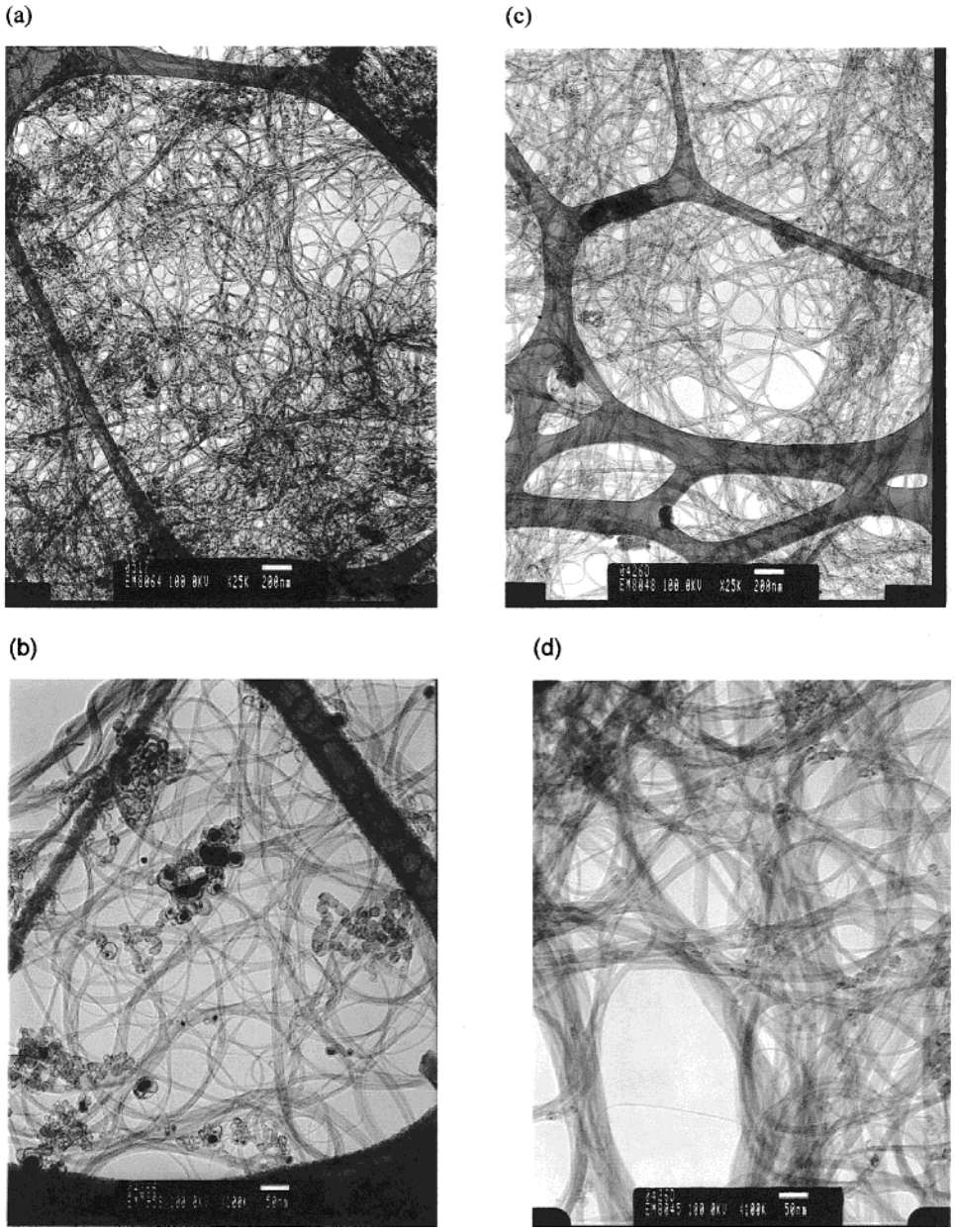

Figure 4. TEM images of SWNTs. Before purification (as-purified Tubes@Rice SWNTs): (a) magnification = 25 000, (b) magnification = 100 000. After two-stage purification process: (c) magnification = 25 000, (d) magnification = 100 000.

oxidation was followed by a wash in concentrated HCl solution. In the first study, the temperature at which the sample was oxidized was raised in small increments in order to determine the temperatures at which the carbon-encased metal is exposed for subsequent reaction with HCl. Typically, the sample was heated in a 5% O_2/Ar, 1 atm mixture, for 1 h at selected temperatures and subsequently sonicated in concentrated HCl for 10 min. The green color that develops in the concentrated HCl provides an indication of the dissolution of cobalt and nickel metal oxides that form during oxidation of the sample. Weight loss after each procedure was determined after drying the samples in vacuum at 150 °C. The temperature at which gas phase oxidation was carried out and the respective weight loss values are given in Table 1. In the second study, the oxidation procedure was reduced to a water reflux and a two-step oxidation process to produce the best results for metal removal with minimum weight loss of nanotubes. In this case, we expose the samples first to 300 °C, then to 500 °C temperature oxidation with an HCl extraction step after each oxidation. Table 2 provides the weight loss and metal concentration data for the two-temperature process. When heated to 500 °C, metal loss is more dramatic, and the final metal content is about 0.1 atomic percent relative to carbon.

Results and Discussion

The rate of oxidation of SWNT samples held at 425 °C in air for 6 h was used as a test of sample purity in the first study. These results are shown in Figure 1. One sees large changes in the rate of oxidation when the sample is refluxed in water and after gas phase oxidation at 300 °C followed by an HCl wash. The next largest change in oxidation rate occurs after gas phase oxidation at 500 °C and an HCl wash. The largest changes in the metal-to-carbon ratio occur after the water reflux, oxidation at 300 and at 500 °C gas phase treatments respectively, and these correlate with the largest changes in the rate of oxidation shown in Figure 1. This clearly suggests that SWNT oxidation at 425 °C is metal catalyzed. From the result in the first study, we adopted the two temperatures, 300 and 500 °C, as the

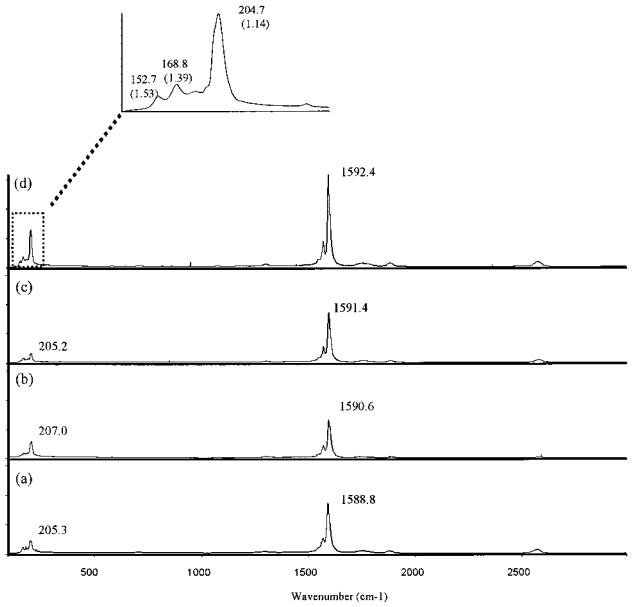

Figure 5. Raman spectra of SWNTs: (a) Tubes@Rice SWNTs raw materals, (b) as-purified Tubes@Rice SWNTs, (c) after two-stage purification process, (d) after two-stage purification and annealing at 900 °C, Inset is the expanded Raman spectra of (d), showing the breathing modes of nanotubes. Diameter value is calculated as $d = 234\ \text{nm}/\nu$, where d is the tube diameter in nanometers and ν is the wavenumber for the peak

oxidation temperatures for the two-stage gas phase purification process in the second study.

Figure 2 illustrates the oxidative behavior of a sample that has been cleaned with the two-stage process. This sample appears to be stable in air at temperatures as high as 550 °C. It is likely that oxidative stability up to 600 °C can be achieved with more metal removal. However, the higher temperature oxidation treatments will also result in the loss of a larger percentage of SWNTs. To verify the catalytic oxidation effects of the metal present in a nanotubes sample we added Co from a $Co(NO_3)_2$ aqueous solution to the cleaned sample. Its oxidative behavior in air is also shown in Figure 2. A reduction in air stability is clearly seen for the Co-doped sample, thus proving that metal catalyzed oxidation of SWNTs occurs at temperatures below 500 °C.

Figures 3 and 4 show SWNT samples before and after the purification process with SEM and TEM, respectively. The bright areas are thought to be due to agglomerated metal particles. They are clearly removed by the cleaning process. In the TEM images shown in Figure 4, metal particles are identified as the dark particles. They appear to be gathered into groups and associated with a nodular form of carbon. In the cleaned sample most of the metal is gone; however, some of the nodular carbon is still present.

Figure 5 shows Raman spectra of SWNTs as raw material, nitric acid treated, purified through the two-stage oxidation process, and purified SWNTs annealed at 900 °C. Typical SWNT features are observed for the tangential and radial modes near 1590 and 180 cm^{-1}, respectively. The most noticeable effect of cleaning and annealing is the increased intensity of the Raman features when the cleaned sample is annealed at 900 °C. The radial modes present near 180 cm^{-1} can be correlated with SWNT diameters.[24−28] The peaks present for the annealed sample suggest that the nanotube diameter in the sample range from 1.13 to 1.53 nm, with an average size of 1.33 nm. This is calculated with $d = 234/\nu$, [29] where d is the tube diameter in nanometers and ν is in wavenumbers.

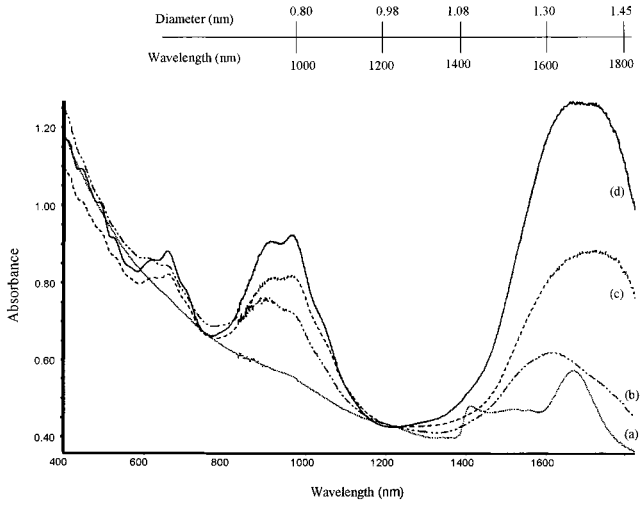

Figure 6. UV−vis−near-IR of purified SWNTs: (a) raw soot, (b) as-purified Tubes@Rice SWNTs, (c) after two-stage purification process, (d) after two-stage purification process and annealing at 900 °C. Spectra have been normalized at 1200 nm. Scale bar shows adjusted tube diameter: d (diameter in nm) $= 2\gamma_0 a_{c-c}/E_g$, where E_g is the semiconducting energy gaps of SWNTs, a_{c-c} is 0.142 nm, and γ_0, the best-fit parameter from experimental STM data,[29] is 2.7 eV. We have converted E_g to λ for the convenience of calculating tube diameter directly from UV−vis−near-IR spectra, and multiply the equation by 1.3 to give the correct average diameter of tubes as determined by X-ray diffraction data. The final form of equation that we use to calculate tube diameters is $d = 8.041 \times 10^{-4}\lambda$, where d and λ are in nanometers.

Figure 6 presents UV−vis−near-IR spectra of SWNTs suspended in a 0.15 wt % Triton-X/D_2O solution. All of the spectra have been normalized to the annealed sample spectral intensity at 1200 nm. Well-spaced and symmetric structures, called van Hove singularities, appear in the local density of states of nanotubes due to the one-dimensional nature of the conduction electron states in nanotubes.[30] The one-dimensional nature of the energy bands has been illustrated previously by observation of the van Hove singularities with STM studies.[31−33] UV−vis−near-IR spectra provide additional evidence of this phenomenon.

The peak centered at 1700 nm is due to the first van Hove singularity in semiconducting nanotubes while the second Van Hove singularity is seen centered at 900 nm. A third set of peaks centered near 650 nm is assigned to the first van Hove transition of metallic SWNTs.[30] The van Hove peaks are superimposed on a background that decreases smoothly from the ultraviolet to the near-infrared.

The location of the van Hove peaks is a sensitive function of the SWNT diameter.[31,34,35] Smaller diameter tubes exhibit van Hove transitions at shorter wavelengths. The observed peaks are due to overlapping van Hove transitions from all nanotube sizes that are present. The dependence of the band gap of semiconducting SWNTs on diameter has been measured with STM by Lieber.[31,34,35] This information permits the prediction of the location of the first van Hove transition in the near-infrared for semiconducting SWNTs. The position is determined by the band gap and the width of the van Hove singularity peak in electron density as a function of energy.[31] Because of the finite width of the van Hove singularity, the optical peak position will appear at a higher energy than the measured band gap.

Thess et al.[21] in 1996 showed that the average diameter of SWNTs produced by Tubes@Rice is 1.38 nm, as determined from X-ray diffraction. In order to correlate the average diameter (1.38 nm) measurement for these laser-oven-grown samples as obtained by X-ray diffraction, we have increased the predicted

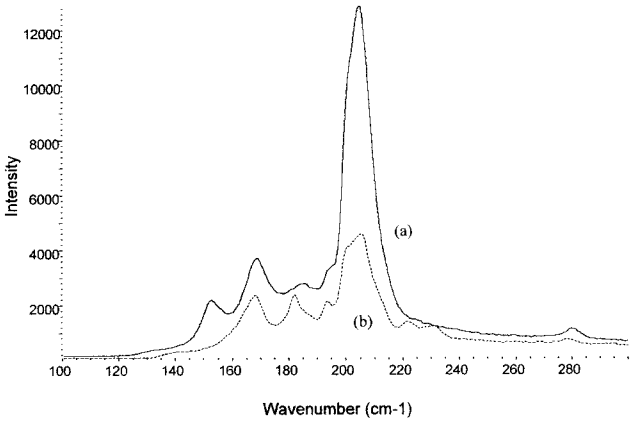

Figure 7. Raman breathing modes of raw and purified single-wall carbon nanotubes: (a) after two-stage purification process and annealing at 900 °C, (b) raw soot. Numbers in parentheses denotes the tube diameter calculated as $d = 234$ nm/ν, where d is the tube diameter in nanometers and ν is the wavenumber for the peak.

diameter from band gap information of Lieber at. el. by 30% to account for the width of the van Hove singularity. The adjusted scale is shown in Figure 6.

It is interesting to note that the first van Hove transition for the material taken directly from the laser-oven-grown raw soot appears quite different from the other spectra. Its appearance suggests that two distributions of nanotube diameters are produced in the Tubes@Rice growth process. We note that the relative intensities of the breathing modes in Raman spectra do not show the same relative intensities for different tube diameters. (Figure 7). We attribute this to differences in resonant enhancement behavior for different SWNT diameters. In fact, Raman spectra do not appear to accurately track relative changes in concentration for different diameters during the cleaning process. We believe that UV−vis−near-IR spectra are a more reliable measure of SWNT size distributions since the transition moments of the van Hove singularities for different diameters are likely to be similar and only weakly dependent on tube diameters.

Subsequent oxidative cleaning with nitric acid and gas phase oxidation appears to remove smaller diameter tubes preferentially. This is evidenced by a shift of the first van Hove peak to longer wavelengths with each cleaning step. It is also seen that the intensities of the van Hove transitions increase with cleaning and annealing of the nanotubes. In fact, the absorbance values at 1700 nm for the cleaned and annealed sample are almost equal to the absorbance at 400 nm. It is interesting to speculate that the relative intensity of the first van Hove transition to the continuum absorbance value at 400 nm in the ultraviolet provides a useful measure of the perturbation of the HOMO π-electron density of SWNTs due to sidewall substitution and/or oxidation. For instance, other studies have shown that the van Hove features are completely absent for partially alkylated SWNTs with retention of the continuum background.[36]

Summary

A purification method has been developed which leads to 99.9% pure single-wall nanotubes with respect to metal content. It combines the well-known acid reflux treatment with water reflux and a two-stage gas phase oxidation process. The air oxidation rate of SWNTs at low temperatures was clearly correlated to the amount of metal in the sample. We also suggest the use of the intensity of the first van Hove transition relative to absorption in the ultraviolet as a qualitative measurement of SWNT sidewall oxidation and/or functionalization.

Acknowledgment. This work was supported by Robert A. Welch Foundation, the Advanced Technology Program of Texas, the National Aeronautics and Space Administration, Office of Naval Research, and the National Science Foundation.

References and Notes

(1) Iijima, S.; Ichihashi, T. *Nature* **1993**, *363*, 603.
(2) Iijima, S.; Ichihashi, T. *Nature (London)* **1993**, *364*, 737.
(3) Issi, J. P.; Langer, L.; Heremans, J.; Olk, C. H. *Carbon* **1995**, *33*, 941.
(4) Cornwell, C. F.; Wille, L. T. *Solid State Commun.* **1997**, *101*, 555−558.
(5) Fuhrer, M. S.; Nygard, J.; Shih, L.; Forero, M.; Yoon, Y. G.; Mazzoni, M. S.; Zetti, A.; McEuen, P. *Science* **2000**, *288*, 294.
(6) Rosen, R.; Simendinger, W.; Debbault, C.; Shimoda, H.; Stoner, L.; Zhou, O. *Appl. Phys. Lett.* **2000**, *76*, 1668.
(7) Smith, B.; Luzzi, D. *Chem. Phys. Lett.* **2000**, *321*, 169.
(8) Hidefumi, H. *Mol. Cryst. Liq. Cryst. Sci. Technol., Sect. A* **1995**, *276*, 267.
(9) Yumura, M.; Uchida, K.; Niino, H.; Ohshima, S.; Kuriki, Y.; Yase, K.; Ikazaki, F. *Mater. Res. Soc. Symp. Proc. Novel Forms of Carbon II* **1994**, *349*, 231.
(10) Dillon, A.; Gennett, T.; Jones, K.; Alleman, J.; Parilla, P.; Heben, M. *Adv. Mater.* **1999**, *16*, 1354.
(11) Bandow, S.; Zhao, X.; Ando, Y. *Appl. Phys. A* **1999**, *67*, 23.
(12) Rinzler, A.; Liu, J.; Dai, H.; Nikolaev, P.; Huffman, C.; Rodriguez-Macias, F.; Boul, P.; Lu, A.; Heymann, D.; Colbert, D. T.; Lee, R. S.; Fischer, J.; Rao, A.; Eklund, P. C.; Smalley, R. E. *Appl. Phys. A* **1998**, *67*, 29.
(13) Dujardin, E.; Ebbesen, T.; Krishnan, A.; Treacy, M. *Adv. Mater.* **1998**, *10*, 611.
(14) Ebbesen, T.; Ajatan, A.; Hiura, H.; Tanigaki, K. *Nature* **1994**, *367*, 519.
(15) Hiura, H.; Ebbesen, T.; Tanigaki, T. *Adv. Mater.* **1995**, *7*, 275.
(16) Dillon, A. C.; Jones, K. M.; Bekkedahl, T. A.; Kiang, C. H.; Bethune, D. S.; Heben, M. J. *Nature* **1997**, *386*, 377.
(17) Zimmerman, J. L.; Bradley, R. K.; Huffman, C. B.; Hauge, R. H.; Margrave, J. L. *Chem. Mater.* **2000**, *12*, 1361.
(18) Bandow, S.; Rao, A. M.; Williams, K. A.; Thess, A.; Smalley, R. E.; Eklund, P. C. *J. Phys. Chem. B* **1997**, *101*, 8839.
(19) Shelimov, K. B.; Esenaliev, R. O.; Rinzler, A. G.; Huffman, C. B.; Smalley, R. E. *Chem. Phys. Lett.* **1998**, *282*, 429.
(20) Duesberg, G. S.; Burghard, M.; Muster, J.; Philipp, J.; Roth, S. *Chem. Commun.* **1998**, *1998*, 435.
(21) Thess, A.; Lee, R.; Nikolaev, P.; Dai, H. J.; Petit, P.; Robert, J.; Xu, C. H.; Lee, Y. H.; Kim, S. G.; Rinzler, A. G.; Colbert, D. T.; Scuseria, G. E.; Tománek, D.; Fischer, J. E.; Smalley, R. E. *Science* **1996**, *273*.
(22) Tohji, K.; Goto, T.; Takahashi, H.; Shinoda, Y.; Shimizu, N.; Jeyadevan, B.; Matsuoka, I.; Saito, Y.; Ohsuna, T. *Proc. Electrochem. Soc. 96−10, Materials* **1996**, *3*, 84.
(23) Tohji, K.; Takahashi, H.; Shinoda, Y.; Shimizu, N.; Jeyadevan, B.; Matsuoka, I.; Saito, Y.; Kasuya, A.; Ito, S.; Nishina, Y. *J. Phys. Chem. B* **1997**, *11*, 1974.
(24) Maeda, T.; Horie, C. *Physica B* **1999**, *263*, 479.
(25) Rao, A. M.; Richter, E.; Bandow, S.; Chase, B.; Eklund, P. C.; Williams, K. A.; Fang, S.; Subbaswamy, K. R.; Menon, M.; Thess, A.; Smalley, R. E.; Dresselhaus, G.; Dresselhaus, M. S. *Science* **1997**, *275*, 187.
(26) Sugano, M.; Kasuya, A.; Tohji, K.; Saito, Y.; Nishina, Y. *Chem. Phys. Lett.* **1998**, *292*, 575.
(27) Duesberg, G. S.; Blau, W. J.; Byrne, H. J.; Muster, J.; Burghard, M.; Roth, S. *Chem. Phys. Lett.* **1999**, *310*, 8.
(28) Saito, R.; Takeya, T.; Kimura, T.; Dresselhaus, G.; Dresselhaus, M. S. *Phys. Rev. B* **1998**, *57*, 4145.
(29) Bandow, S.; Asaka, S.; Saito, Y.; Rao, A.; Grigorian, L.; Richter, E.; Eklund, P. C. *Phys. Rev. B: Condens. Matter* **1998**, *80*, 3779.
(30) Kim, P.; Odom, T. W.; Huang, J.; Lieber, C. M. *Phys. Rev. Lett.* **1999**, *82*, 1225.
(31) Wildoer, J. W.; Venema, L. C.; Rinzler, A. G.; Smalley, R. E.; Dekker, C. *Nature* **1998**, *391*, 59.
(32) Dekker, C. *Phys. Today* **1999**, *May*, 22.
(33) Ajayan, P. J. *Chem. Rev.* **1999**, *99*, 1787.
(34) Wirth, I.; Eisebitt, S.; Kann, G.; Eberhardt, W. *Phys. Rev. B* **2000**, *61*, 5719.
(35) Odom, T. W.; Huang, J. L.; Kim, P.; Lieber, C. M. *Nature* **1998**, *391*, 62.
(36) Boul, P. J.; Liu, J.; Mickelson, E. T.; Huffman, C. B.; Ericson, L. M.; Chiang, I. W.; Smith, K. A.; Colbert, D. T.; Hauge, R. H.; Margrave, J. L.; Smalley, R. E. *Chem. Phys. Lett* **1999**, *310*, 367.